# A Nearly Linear Single Hydroxo Bridge. Synthesis, Structure, and Magnetic Susceptibility of ($\mu$-Hydroxo)bis((tetraphenylporphinato)manganese(III)) Perchlorate

**Beisong Cheng,[1a] Pascal H. Fries,*[,1b] Jean-Claude Marchon,*[,1b] and W. Robert Scheidt*[,1a]**

Department of Chemistry and Biochemistry, University of Notre Dame, Notre Dame, Indiana 46556, and CEA/Département de Recherche Fondamentale sur le Matière Condensée/SESAM and CNRS/Laboratoire de Chimie de Coordination (Unité de Recherche Associée No. 1194), Centre d'Études Nucléaires de Grenoble, 38054 Grenoble Cedex, France

*Received August 9, 1995*[⊗]

The synthesis, X-ray structure, and magnetic susceptibility characterization of a hydroxo-bridged complex, ($\mu$-hydroxo)bis((tetraphenylporphinato)manganese(III)) perchlorate, {[Mn-(TPP)]$_2$(OH)}ClO$_4$, are described. The complex is readily prepared by a controlled hydrolysis of monomeric diaquo(tetraphenylporphinato)manganese-(III) perchlorate. Interestingly, the bridging hydroxo complex appears to be more stable than the putative $\mu$-oxo complex in halocarbon solvents. The X-ray structure determination shows a complex in which two five-coordinate manganese(III) ions are bridged by a single hydroxo ligand with an average Mn−O distance of 2.026(1) Å and a Mn−O(H)−Mn bridge angle of 160.4(8)°. The two porphyrin planes are nearly coplanar, and the two metal ions are separated by 3.993 Å. The average Mn−N$_P$ distance is 2.008(7) Å. The two manganese ions are displaced by 0.19 and 0.20 Å from their respective 24-atom mean planes. Both of the two porphyrin rings are moderately $S_4$ ruffled and have a near-staggered orientation (the N−Mn−Mn′−N′ dihedral angle is 29.9°). The four inter-ring pairs of *meso*-phenyl groups of the binuclear cation are extremely crowded, with a nearly perpendicular orientation for each pair. The solid-state magnetic susceptibility was measured over the temperature range 2−300 K. The observed behavior is typical of an exchange-coupled binuclear complex. The data were fit to the total spin Hamiltonian ($H_{tot} = H(1) + H(2) - 2J\bar{S}_1 \cdot \bar{S}_2$) of a zero-field-split, high-spin d$^4$−d$^4$ dimer in its actual crystallographic geometry, using numerical techniques. The hydroxide bridge supports a relatively strong antiferromagnetic coupling ($2J = -74.0$ cm$^{-1}$) between two zero-field-split ($D = -10.8$ cm$^{-1}$) manganese(III) ions. Crystal data: $a = 16.807(7)$ Å, $b = 17.061(6)$ Å, $c = 17.191(5)$ Å, $\alpha = 85.64(3)°$, $\beta = 79.75(3)°$, $\gamma = 61.95(2)°$, triclinic, space group $P\bar{1}$, $V = 4281(3)$ Å$^3$, $Z = 2$, $R_1 = 0.0707$ for 14 802 observed data based on $F_o \geq 4.0\sigma(F_o)$, $R_{2w} = 0.2007$ for 21 696 total unique data, least-squares refinement on $F^2$ using all data.

## Introduction

Multinuclear manganese systems, probably involving oxo and/or hydroxo bridging motifs, are an essential component in a number of metalloenzymes.[2−5] In these bridged systems, the protonation and deprotonation of the oxo bridge may be important in the catalytic cycle of the redox enzymes. Recently, Naruta et al.[6] reported that a binuclear Mn(III) porphyrin complex can lead to oxygen evolution from water. An essential feature of their proposed mechanism is the formation of hydroxide complexes of the porphyrin dimer. The electronic structure and the interaction between manganese centers are thus of some considerable interest, and the synthesis and characterization of manganese complexes with well-defined and simple bridging ligand systems seem to be especially so.

We previously communicated[7] that the $\mu$-oxo iron(III) porphyrinate [Fe(OEP)]$_2$O[8] can be protonated to form the novel single-hydroxo-bridged complex {[Fe(OEP)]$_2$(OH)}ClO$_4$. Recently, we reported[9] that the analogous manganese(III) $\mu$-hydroxo derivative {[Mn(OEP)]$_2$(OH)}ClO$_4$ can be synthesized by controlled hydrolysis of the monomeric precursor [Mn(OEP)-(H$_2$O)]ClO$_4$ or [Mn(OEP)(OClO$_3$)]. It is interesting to note that the $\mu$-oxo species [Mn(OEP)]$_2$O cannot be isolated in crystalline form and is very unstable in halocarbon solvents, while its protonated form is readily obtained and quite stable in halocarbon solvents. Most importantly, the hydroxide bridging ligand is found to mediate an unprecedentedly large antiferromagnetic coupling ($2J = -71.0$ cm$^{-1}$) between the two manganese(III) ions. We have carried out parallel studies on the much more hindered tetraphenylporphyrin system. Herein, we report the detailed synthesis, X-ray structure, and temperature-dependent magnetic susceptibility characterization of the hydroxo-bridged tetraphenylporphyrin analog {[Mn(TPP)]$_2$-(OH)}ClO$_4$.

[⊗] Abstract published in *Advance ACS Abstracts,* January 15, 1996.

(1) (a) University of Notre Dame. (b) Centre d'Études Nucléaires de Grenoble.
(2) *Manganese Redox Enzymes*; Pecoraro, V. L., Ed.; VCH: New York, 1992.
(3) Que, L., Jr.; True, A. E. In *Progress in Inorganic Chemistry: Bioinorganic Chemistry*; Lippard, S. J., Ed.; Interscience: New York, 1990; Vol. 38, Chapter 3.
(4) Wieghardt, K. *Angew. Chem., Int. Ed. Engl.* **1989**, *28*, 1153.
(5) Brudvig, G. W. In *Metal Clusters in Proteins*; Que, L., Jr., Ed.; ACS Symposium Series 372; American Chemical Society: Washington, DC, 1988; pp 221−237. Christou, G.; Vincent, J. B. In *Metal Clusters in Proteins*; Que, L., Jr., Ed.; ACS Symposium Series 372; American Chemical Society: Washington, DC, 1988; pp 238−255.
(6) Naruta, Y.; Sasayama, M.-A.; Sasaki, T. *Angew. Chem., Int. Ed. Engl.* **1994**, *33*, 1839.
(7) Scheidt, W. R.; Cheng, B.; Safo, M. K.; Cukiernik, F.; Marchon, J.-C.; Debrunner, P. G. *J. Am. Chem. Soc.* **1992**, *114*, 4420.
(8) Abbreviations used in this paper: OEP, octaethylporphyrin dianion; TPP, 5,10,15,20-tetraphenylporphyrin dianion; TF$_5$PP, 5,10,15,20-tetrakis(pentafluorophenyl)porphyrin dianion; TMPyP, 5,10,15,20-tetrakis(1-methylpyridinium-4-yl)porphyrin dianion; NCH$_3$TPP, *N*-methyl-*meso*-tetraphenylporphyrin monoanion; TPC, 5,10,15,20-tetraphenylchlorin dianion; FF, face-to-face porphyrin dianion; TTP, 5,10,15,20-tetratolylporphyrin dianion; *sad*, the $S_4$-ruffled conformation of the porphinato ring; N$_p$, porphinato nitrogen atom; Ct, center of the porphyrin ring.
(9) Cheng, B.; Cukiernik, F.; Fries, P. H.; Marchon, J.-C.; Scheidt, W. R. *Inorg. Chem.* **1995**, *34*, 4627.

0020-1669/96/1335-1024$12.00/0 

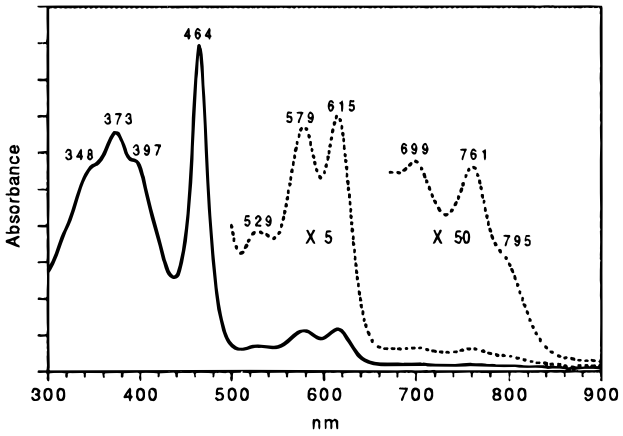


**Figure 1.** UV/vis/near-IR spectrum of $\{[Mn(TPP)]_2(OH)\}ClO_4$ in $CH_2Cl_2$ solution.

## Experimental Section

**General Information.** $H_2TPP$ was prepared by literature methods.[10] Manganese acetate was purchased from Alfa, $HClO_4$ and $CDCl_3$ (chloroform-*d*, 99.8 atom % D) were from Aldrich, and all other reagents were obtained from Fisher. All these materials were used as received unless otherwise noted. Coaxial NMR tubes for solution magnetic susceptibility measurements were bought from Wilmad Glass. IR spectra were recorded on a Perkin-Elmer 883 infrared spectrophotometer as CsBr pellets; electronic spectra were recorded on a Perkin-Elmer Lambda 19 UV/vis/near-IR spectrometer, and NMR spectra were recorded on a General Electric GN300 spectrometer.

**Synthetic Procedures. [Mn(TPP)Cl].** Preparation of [Mn(TPP)Cl] followed our reported[9] procedure for [Mn(OEP)Cl], which was a modification of Adler's preparation.[11] IR ($\nu_{Mn-Cl}$): 291 (m) $cm^{-1}$ (CsBr pellet). UV/vis: $\lambda_{max}$ 346, 374, 400, 477 (Soret), 528, 583, 618 nm.

**$[Mn(TPP)(H_2O)_2]ClO_4$.** A $CH_2Cl_2$ solution (50 mL) of [Mn(TPP)Cl] (0.5 g) was vigorously shaken with 200 mL of aqueous KOH (2 M) twice in a separatory funnel. The $CH_2Cl_2$ layer was separated from the mixture and washed with 200 mL of distilled water twice. The resulting $CH_2Cl_2$ solution was then treated with aqueous $HClO_4$ (~4%, 200 mL). The $CH_2Cl_2$ phase was collected, dried with $Na_2SO_4$, and taken to dryness under vacuum. UV/vis: $\lambda_{max}$ 335, 388, 412 (sh), 478 (Soret), 571, 604 nm.

*Caution!* Although we have experienced no problem with the procedures described in dealing with systems containing perchlorate ion, they can detonate spontaneously and should be handled only in small quantities; in no case should such a system be heated above 30 °C, and other safety precautions are also warranted.[12]

**$\{[Mn(TPP)]_2(OH)\}ClO_4$.** A $CH_2Cl_2$ solution (20 mL) of $[Mn(TPP)(H_2O)_2]ClO_4$ (200 mg) was washed with distilled water (100 mL) five times. An UV/vis spectrum was taken after each washing. Water washes were continued until the blue shift of the Soret band from 478 to 464 nm was *just* complete. The $CH_2Cl_2$ phase was separated from the mixture, dried with $Na_2SO_4$, and taken to dryness. Single crystals were obtained by a liquid diffusion crystallization from $CH_2Cl_2$ and hexanes (5 days).[13] An X-ray structure determination identified the complex as $\{[Mn(TPP)]_2(OH)\}ClO_4$ with solvated $CH_2Cl_2$ and water molecules. UV/vis ($CH_2Cl_2$): $\lambda_{max}$ ($\epsilon$, $cm^{-1}$ $M^{-1}$) 348 ($7.75 \times 10^4$), 373 ($9.02 \times 10^4$), 397 ($7.91 \times 10^4$), 464 ($1.21 \times 10^5$), 529 ($7.50 \times 10^3$), 579 ($1.32 \times 10^4$), 615 ($1.38 \times 10^4$), 699 (933), 761 (911), 795 (511) nm. A typical UV/vis/near-IR spectrum is given in Figure 1.

**X-ray Structure Determination.** Crystals with two different shapes (needle and plate) were isolated from the same crystallization batch. Both crystal types have identical electronic spectra and unit cell parameters.[14] A black, platelike crystal with the dimensions of 0.10 × 0.35 × 0.55 mm was employed for X-ray structure determination on an Enraf-Nonius FAST area-detector diffractometer with a graphite-monochromated Mo rotating anode source ($\bar{\lambda}$ = 0.710 73 Å). Our detailed methods and procedures for small-molecule X-ray data collection with the FAST system were described previously.[15] Both cell determination and intensity data collection were executed at 127(2) K. Any crystal decay problem was excluded by comparison of a common portion of data collected after each sweep during data collection. Data were corrected for Lorentz and polarization factors, and at the final stages of analysis, a modified version[16] of the absorption correction program DIFABS was applied. A brief summary of the crystal data is listed in Table 1, complete crystallographic details are included in the Supporting Information (Table S1). In all tables, the atom names of porphyrin ring 1 of the dimer are preceded by the numeral "1" and those of ring 2 by "2".

**Table 1.** Crystallographic Data for $\{[Mn(TPP)]_2OH\}ClO_4 \cdot 0.84H_2O \cdot 4.65CH_2Cl_2$

| | |
|---|---|
| chem formula: $C_{92.65}H_{68.0}Cl_{10.31}Mn_2N_8O_{5.84}$ | $Z = 2$ |
| $a = 16.807(7)$ Å | space group = $P\bar{1}$ |
| $b = 17.061(6)$ Å | $T = -146(2)$ °C |
| $c = 17.191(5)$ Å | $\lambda = 0.710\ 73$ Å |
| $\alpha = 85.64(3)°$ | $\rho_{calc} = 1.445$ g $cm^{-3}$ |
| $\beta = 79.75(3)°$ | $\mu = 0.68$ $mm^{-1}$ |
| $\gamma = 61.95(2)°$ | $R_1^{20} = 0.0707$ |
| $V = 4281(3)$ Å$^3$ | $R_{2w}^{20} = 0.1710$ |

The structure was solved in the centrosymmetric space group $P\bar{1}$ with the direct-methods program SHELXS-86,[18] and difference Fourier syntheses led to the location of all the remaining non-hydrogen atoms. The structure was refined against $F^2$ with the program SHELXL-93.[19] All data collected were used, including negative intensities. Severe disorder was observed for some solvate components in the lattice corresponding to six different solvent molecule sites. The first $CH_2Cl_2$ molecule (Cl(2)−C(1)−Cl(3)) was ordered with full occupancy. The second $CH_2Cl_2$ (Cl(4)−C(2)−Cl(5)) was also ordered but with an occupancy of 0.725(4). The third $CH_2Cl_2$ was disordered, and two geometries (Cl(6a)−C(3a)−Cl(7a) and Cl(6b)−C(3b)−Cl(7b)) were resolved with occupancies of 0.316(4) and 0.684(4), respectively. Each of the fourth and fifth $CH_2Cl_2$ molecules (Cl(8)−C(4)−Cl(9) and (Cl(10)−C(5)−Cl(11)) were found together with residual density assigned as water molecules (O(w1), O(w2) and O(w3), O(w4), respectively). Thus constraint that the occupancy summation equal 1 for each group was applied, which led to occupancies of 0.543(5), 0.214(9), and 0.243(10) for the fourth $CH_2Cl_2$, O(w1), and O(w2), respectively, and of 0.614(4), 0.176(15), and 0.211(15) for the fifth $CH_2Cl_2$, O(w3), and O(w4), respectively. The sixth $CH_2Cl_2$ (Cl(12)−C(6)−Cl(13)) was found near a symmetry center with a shortest distance of ~1.5 Å for two symmetry-related chlorine atoms (Cl(12)···Cl(12′); therefore, its occupancy cannot be larger than 0.5. An alternative $CH_2Cl_2$ (Cl(14)−C(7)−Cl(15)) was found with close contact to the sixth $CH_2Cl_2$ and one of the fragments of the disordered third $CH_2Cl_2$ (Cl(6b)−C(3b)−Cl(7b)), with distance of 0.483 Å for C(7)···Cl(13) and 2.505 Å for Cl(14)···Cl(7b). Thus, the occupancy of the sixth $CH_2Cl_2$ was refined independently to be 0.456(4) and that of the seventh $CH_2Cl_2$ was assumed to be the same as that of Cl(6a)−C(3a)−Cl(7a) and refined in the least-squares process. Although there may be other alternatives in interpreting these concerted disorder problems, our detailed examination considered the geometry, the thermal motion, the nonbonding interactions, the difference Fouriers, and the behavior in least-squares

(10) Adler, A. D.; Longo, F. R.; Finarelli, J. D.; Goldmacher, J.; Assour, J.; Korsakoff, L. *J. Org. Chem.* **1967**, *32*, 476.
(11) Adler, A. D.; Longo, F. R.; Kampas, F.; Kim, J. *J. Inorg. Nucl. Chem.* **1970**, *32*, 2443.
(12) Wolsey, W. C. *J. Chem. Educ.* **1973**, *50*, A335. *Chem. Eng. News* **1983**, *61* (Dec 5), 4; **1963**, *41* (July 8), 47.
(13) If the crystallization time was too long, *e.g.* 10 days, a crystalline [Mn(TPP)Cl] impurity was noted.
(14) Crystals obtained from $CH_2Cl_2$ and hexanes were extremely unstable largerly because of the $CH_2Cl_2$ solvate. In order to find a satisfactory X-ray-quality single crystal, a total of eight crystals with different shapes were examined on the diffractometer, all of which gave a constant set of unit cell parameters.
(15) Scheidt, W. R.; Turowska-Tyrk, I. *Inorg. Chem.* **1994**, *33*, 1314.
(16) The process is based on an adaptation of the DIFABS[17] logic to area detector geometry by: Karaulov, A. I. School of Chemistry and Applied Chemistry, University of Wales College of Cardiff, Cardiff CF1 3TB, U.K. Personal communication.
(17) Walker, N. P.; Stuart, D. *Acta Crystallogr., Sect. A* **1983**, *A39*, 158.
(18) Sheldrick, G. M. *Acta Crystallogr., Sect. A* **1990**, *A46*, 467.
(19) Sheldrick, G. M. *J. Appl. Crystallogr.* in press.

**Table 2.** Atomic Coordinates and Equivalent Isotropic Displacement Parameters (Å$^2$) for $\{[Mn(TPP)]_2OH\}ClO_4 \cdot 0.84H_2O \cdot 4.65CH_2Cl_2$[a]

| atom | *x* | *y* | *z* | *U*(eq) | atom | *x* | *y* | *z* | *U*(eq) |
|---|---|---|---|---|---|---|---|---|---|
| Mn(1) | 0.11922(3) | 0.32982(3) | 0.49845(3) | 0.0190(1) | 2C(b6) | 0.4309(3) | 0.2752(2) | 0.2625(2) | 0.247(7) |
| 1N(1) | 0.0997(2) | 0.3619(2) | 0.6122(2) | 0.0221(6) | 2C(b7) | 0.4708(3) | 0.3763(3) | 0.5119(2) | 0.0264(7) |
| 1N(2) | 0.0859(2) | 0.2320(2) | 0.5314(2) | 0.0229(6) | 2C(b8) | 0.4573(3) | 0.3564(3) | 0.5891(2) | 0.0281(7) |
| 1N(3) | 0.1133(2) | 0.3130(2) | 0.3857(2) | 0.0205(5) | 2C(m1) | 0.3952(2) | 0.2608(2) | 0.6648(2) | 0.0226(6) |
| 1N(4) | 0.1208(2) | 0.4454(2) | 0.4669(2) | 0.0219(6) | 2C(m2) | 0.3407(2) | 0.0220(2) | 0.5939(2) | 0.0207(6) |
| 1C(a1) | 0.1217(2) | 0.4226(2) | 0.6403(2) | 0.0239(7) | 2C(m3) | 0.4176(2) | 0.0742(2) | 0.3161(2) | 0.0209(6) |
| 1C(a2) | 0.0921(2) | 0.3103(2) | 0.6762(2) | 0.0242(7) | 2C(m4) | 0.4473(2) | 0.3290(2) | 0.3871(2) | 0.0213(6) |
| 1C(a3) | 0.0595(2) | 0.2109(2) | 0.6076(2) | 0.0243(7) | 2C(11) | 0.3928(3) | 0.2997(2) | 0.7408(2) | 0.0239(7) |
| 1C(a4) | 0.0712(2) | 0.1814(2) | 0.4823(2) | 0.0250(7) | 2C(12) | 0.3360(3) | 0.3892(2) | 0.7579(2) | 0.0263(7) |
| 1C(a5) | 0.1181(2) | 0.2374(2) | 0.3565(2) | 0.0238(7) | 2C(13) | 0.3310(3) | 0.4248(3) | 0.8298(2) | 0.0330(8) |
| 1C(a6) | 0.1399(2) | 0.3536(2) | 0.3211(2) | 0.0214(6) | 2C(14) | 0.3837(3) | 0.3712(3) | 0.8845(2) | 0.0359(9) |
| 1C(a7) | 0.1244(2) | 0.4804(2) | 0.3921(2) | 0.0226(6) | 2C(15) | 0.4408(3) | 0.2823(3) | 0.8682(2) | 0.0343(9) |
| 1C(a8) | 0.1211(2) | 0.5053(2) | 0.5167(2) | 0.0210(6) | 2C(16) | 0.4455(3) | 0.2458(3) | 0.7963(2) | 0.0276(7) |
| 1C(b1) | 0.1307(2) | 0.4055(3) | 0.7220(2) | 0.0271(7) | 2C(21) | 0.3054(2) | −0.0377(2) | 0.6356(2) | 0.0228(7) |
| 1C(b2) | 0.1117(2) | 0.3381(2) | 0.7440(2) | 0.0260(7) | 2C(22) | 0.2349(2) | −0.0441(2) | 0.6096(2) | 0.0255(7) |
| 1C(b3) | 0.0256(3) | 0.1486(3) | 0.6053(2) | 0.0299(8) | 2C(23) | 0.1969(3) | −0.0950(3) | 0.6503(2) | 0.0307(8) |
| 1C(b4) | 0.0337(3) | 0.1298(2) | 0.5281(2) | 0.0290(8) | 2C(24) | 0.2302(3) | −0.1411(2) | 0.7176(2) | 0.0331(9) |
| 1C(b5) | 0.1506(3) | 0.2304(3) | 0.2735(2) | 0.0296(8) | 2C(25) | 0.3008(3) | −0.1361(2) | 0.7434(2) | 0.0303(8) |
| 1C(b6) | 0.1655(3) | 0.3002(2) | 0.2521(2) | 0.0267(7) | 2C(26) | 0.3388(3) | −0.0852(2) | 0.7027(2) | 0.0251(7) |
| 1C(b7) | 0.1202(3) | 0.5659(2) | 0.3964(2) | 0.0264(7) | 2C(31) | 0.4197(3) | 0.0344(2) | 0.2408(2) | 0.0244(7) |
| 1C(b8) | 0.1182(2) | 0.5810(2) | 0.4731(2) | 0.0251(7) | 2C(32) | 0.4925(3) | 0.0125(2) | 0.1796(2) | 0.0281(7) |
| 1C(m1) | 0.1303(2) | 0.4908(2) | 0.5967(2) | 0.0217(6) | 2C(33) | 0.4934(3) | −0.0238(3) | 0.1096(2) | 0.0367(9) |
| 1C(m2) | 0.0673(2) | 0.2431(2) | 0.6763(2) | 0.0261(7) | 2C(34) | 0.4220(4) | −0.0382(3) | 0.1000(2) | 0.0421(11) |
| 1C(m3) | 0.0921(2) | 0.1789(2) | 0.4002(2) | 0.0249(7) | 2C(35) | 0.3488(3) | −0.0168(3) | 0.1604(3) | 0.0397(10) |
| 1C(m4) | 0.1400(2) | 0.4347(2) | 0.3224(2) | 0.0229(6) | 2C(36) | 0.3479(3) | 0.0191(2) | 0.2310(2) | 0.0297(8) |
| 1C(11) | 0.1584(2) | 0.5479(2) | 0.6339(2) | 0.0239&) | 2C(41) | 0.4586(2) | 0.4028(2) | 0.3434(2) | 0.0221(6) |
| 1C(12) | 0.1093(3) | 0.5977(2) | 0.7021(2) | 0.0295(8) | 2C(42) | 0.5311(3) | 0.3872(2) | 0.2830(2) | 0.0263(7) |
| 1C(13) | 0.1445(3) | 0.6409(3) | 0.7394(2) | 0.356(9) | 2C(43) | 0.5391(3) | 0.4571(3) | 0.2423(2) | 0.0296(8) |
| 1C(14) | 0.2275(3) | 0.6368(3) | 0.7081(2) | 0.0365(9) | 2C(44) | 0.4742(3) | 0.5435(3) | 0.2614(2) | 0.0311(8) |
| 1C(15) | 0.2763(3) | 0.5894(3) | 0.6386(2) | 0.0360(9) | 2C(45) | 0.4016(3) | 0.5603(2) | 0.3217(2) | 0.0310(8) |
| 1C(16) | 0.2416(3) | 0.5459(2) | 0.6020(2) | 0.0280(7) | 2C(46) | 0.3937(3) | 0.4903(2) | 0.3626(2) | 0.0257(7) |
| 1C(21) | 0.0459(3) | 0.2064(3) | 0.7539(2) | 0.0274(7) | O(1a)[b] | 0.2583(3) | 0.2715(6) | 0.4852(4) | 0.022(2) |
| 1C(22) | −0.0188(3) | 0.2632(3) | 0.8140(2) | 0.0322(8) | O(1b)[c] | 0.2549(6) | 0.2518(12) | 0.4750(7) | 0.027(3) |
| 1C(23) | −0.0398(3) | 0.2303(3) | 0.8858(2) | 0.0404(10) | H(1) | 0.2682(37) | 0.2796(38) | 0.4429(34) | 0.050 |
| 1C(24) | 0.0019(3) | 0.1396(3) | 0.8995(2) | 0.0434(11) | C1(1) | 0.22320(7) | 0.71673(7) | 0.92002(5) | 0.0362(2) |
| 1C(25) | 0.0655(3) | 0.0824(3) | 0.8401(2) | 0.0392(9) | O(2) | 0.2373(3) | 0.7314(3) | 0.9959(2) | 0.0702(12) |
| 1C(26) | 0.0875(3) | 0.1158(3) | 0.7681(2) | 0.0330(8) | O(3) | 0.2969(2) | 0.7109(2) | 0.8612(2) | 0.0442(7) |
| 1C(31) | 0.0854(3) | 0.1108(2) | 0.3557(2) | 0.0251(7) | O(4) | 0.2196(4) | 0.6351(3) | 0.9221(2) | 0.0772(14) |
| 1C(32) | 0.1366(3) | 0.0206(3) | 0.3686(2) | 0.0316(8) | O(5) | 0.1412(3) | 0.7871(3) | 0.9012(3) | 0.0816(14) |
| 1C(33) | 0.1311(3) | −0.0412(3) | 0.3245(2) | 0.0394(10) | C(1) | 0.2322(4) | 0.7517(4) | 1.1709(3) | 0.0562(14) |
| 1C(34) | 0.0747(3) | −0.0133(3) | 0.2682(2) | 0.0393(10) | C1(2) | 0.18996(7) | 0.73528(7) | 1.26930(6) | 0.0359(2) |
| 1C(35) | 0.0234(3) | 0.0751(3) | 0.2550(2) | 0.0374(9) | C1(3) | 0.32802(10) | 0.76764(12) | 1.16629(10) | 0.0707(4) |
| 1C(36) | 0.0283(3) | 0.1372(3) | 0.2988(2) | 0.0331(8) | C(2)[d] | 0.2934(5) | 0.7414(5) | 0.4855(4) | 0.052(2) |
| 1C(41) | 0.1640(3) | 0.4714(2) | 0.2457(2) | 0.0262(7) | C1(4)[d] | 0.32576(12) | 0.78926(10) | 0.40019(12) | 0.0535(6) |
| 1C(42) | 0.1152(3) | 0.4857(3) | 0.1836(2) | 0.0334(8) | C1(5)[d] | 0.17627(13) | 0.77050(12) | 0.49789(14) | 0.0605(6) |
| 1C(43) | 0.1431(4) | 0.5136(3) | 0.1111(2) | 0.0441(11) | C(3a)[e] | 0.2063(19) | 0.9524(20) | 0.9726(17) | 0.137(19) |
| 1C(44) | 0.2173(4) | 0.5304(3) | 0.0995(3) | 0.0539(14) | C1(6a)[e] | 0.1307(7) | 0.9981(6) | 1.0607(5) | 0.099(2) |
| 1C(45) | 0.2646(4) | 0.5184(4) | 0.1609(3) | 0.0517(13) | C1(7a)[e] | 0.2543(5) | 1.0281(5) | 0.9410(4) | 0.079(2) |
| 1C(46) | 0.2383(3) | 0.4891(3) | 0.2336(2) | 0.0364(9) | C((3b)[f] | 0.2468(8) | 0.9089(9) | 0.9723(6) | 0.066(3) |
| Mn(2) | 0.38791(3) | 0.17894(3) | 0.49056(3) | 0.0177(1) | Cl(6b)[f] | 0.1647(2) | 0.9698(2) | 1.0492(2) | 0.0724(7) |
| 2N(1) | 0.3719(2) | 0.1475(2) | 0.6048(2) | 0.0210(5) | Cl(7b)[f] | 0.3069(3) | 0.9645(4) | 0.92450(15) | 0.104(2) |
| 2N(2) | 0.3887(2) | 0.0670(2) | 0.4615(2) | 0.0204(5) | C(4)[g] | 0.0075(7) | 0.6714(9) | −0.0474(5) | 0.061(3) |
| 2N(3) | 0.4293(2) | 0.1943(2) | 0.3762(2) | 0.0194(5) | Cl(8)[g] | 0.0264(3) | 0.5761(3) | −0.0802(2) | 0.0707(12) |
| 2N(4) | 0.4208(2) | 0.2714(2) | 0.5196(2) | 0.0210(5) | Cl(9)[g] | −0.0670(2) | 0.7662(3) | −0.0979(2) | 0.0874(14) |
| 2C(a1) | 0.3657(2) | 0.1972(2) | 0.6680(2) | 0.0213(6) | C(5)[h] | 0.2429(6) | 0.2976(6) | 0.0158(4) | 0.051(2) |
| 2C(a2) | 0.3386(2) | 0.0899(2) | 0.6359(2) | 0.0218(6) | Cl(10)[h] | 0.3167(2) | 0.1982(2) | 0.05037(13) | 0.0643(8) |
| 2C(a3) | 0.3720(2) | 0.0087(2) | 0.5131(2) | 0.0213(6) | Cl(11)[h] | 0.2072(2) | 0.2918(2) | −0.07054(12) | 0.0737(9) |
| 2C(a4) | 0.4075(2) | 0.0315(2) | 0.3867(2) | 0.0221(6) | C(6)[i] | 0.4567(10) | −0.3976(10) | −0.0157(12) | 0.092(5) |
| 2C(a5) | 0.4222(2) | 0.1537(2) | 0.3130(2) | 0.0210(6) | Cl(12)[i] | 0.5454(3) | −0.5016(3) | −0.0081(3) | 0.093(2) |
| 2C(a6) | 0.4353(2) | 0.2692(2) | 0.3455(2) | 0.0211(6) | Cl(13)[i] | 0.4878(5) | −0.3178(4) | −0.0561(2) | 0.0758(14) |
| 2C(a7) | 0.4465(2) | 0.3239(2) | 0.4685(2) | 0.0223(6) | C(7)[j] | 0.4569(19) | −0.2969(16) | −0.0451(24) | 0.093(17) |
| 2C(a8) | 0.4241(2) | 0.2932(2) | 0.5945(2) | 0.0233(7) | Cl(14)[j] | 0.4355(4) | −0.1874(3) | −0.0611(2) | 0.0593(14) |
| 2C(b1) | 0.3265(2) | 0.1703(2) | 0.7390(2) | 0.0236(7) | Cl(15)[j] | 0.5728(3) | −0.3712(4) | −0.0778(2) | 0.0606(15) |
| 2C(b2) | 0.3086(2) | 0.1056(2) | 0.7190(2) | 0.0244(7) | O(w1)[k] | −0.0504(9) | 0.7057(10) | −0.1172(7) | 0.029(4) |
| 2C(b3) | 0.3865(2) | −0.0672(2) | 0.4704(2) | 0.0236(7) | O(w2)[l] | 0.0760(10) | 0.5248(10) | −0.0873(8) | 0.034(3) |
| 2C(b4) | 0.4085(2) | −0.0524(2) | 0.3928(2) | 0.0239(7) | O(w3)[m] | 0.2691(19) | 0.2130(18) | −0.0243(15) | 0.073(10) |
| 2C(b5) | 0.4225(3) | 0.2047(2) | 0.2427(2) | 0.0242(7) | O(w4)[n] | 0.1823(32) | 0.2245(28) | −0.0175(25) | 0.157(19) |

[a] The estimated standard deviations of the least significant digits are given in parentheses. *U*(eq) is defined as one-third of the trace of the orthogonalized $\mathbf{U}_{ij}$ tensor. [b] Occupancy number 0.62(4). [c] Occupancy number 0.38(4). [d] Occupancy number 0.725(4). [e] Occupancy number 0.316(4). [f] Occupancy number 0.684(4). [g] Occupancy number 0.543(5). [h] Occupancy number 0.614(4). [i] Occupancy number 0.456(5). [j] Occupancy number 0.316(4). [k] Occupancy number 0.214(9). [l] Occupancy number 0.24(1). [m] Occupancy number 0.18(2). [n] Occupancy number 0.21(2).

refinement, and we believe that the currently presented model is the best possible one. Constraint of the C−Cl bond lengths (with "DFIX 1.75" in SHELXL-93) was applied to the third, sixth, and seventh $CH_2Cl_2$ molecules. Atoms Cl(6a), Cl(6b), and C(7) and the four partial

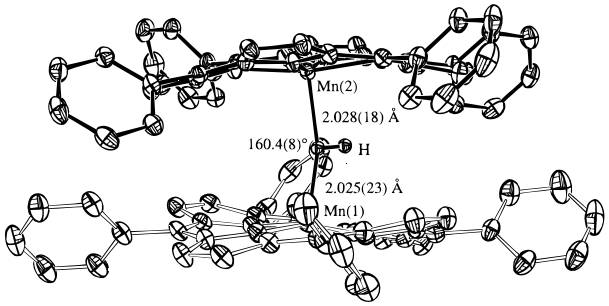


**Figure 2.** "Edge-view" ORTEP diagram of $\{[Mn(TPP)]_2(OH)\}^+$. Thermal ellipsoids are drawn at the 50% probability level. Porphyrin hydrogen atoms are omitted for clarity. The two disordered positions for the $\mu$-hydroxo bridge oxygen atom are nearly overlapped with each other. Thermal parameters for the $\mu$-hydroxo group are reduced.

water oxygens were treated as isotropic contributors. Hydrogen atoms of the two porphyrin ligands and ordered $CH_2Cl_2$ solvates were idealized with the standard SHELXL-93 idealization methods.

At the final stage of the least-squares refinement, it was noted that the bridging hydroxo oxygen atom had an unusual thermal ellipsoid and residual electron density within 0.8 Å. Thus an isotropic, two-site model (O(1a) and O(1b)) was used to describe the bridging oxygen atom with a refined separation of ~0.42 Å and occupancies of 0.62(4) and 0.38(4), respectively. The $\mu$-hydroxo hydrogen atom was directly located from the difference Fourier; its coordinates were refined in least-squares but the isotropic thermal parameter was fixed at 0.05.

At convergence, the discrepancy indices[20] are $R_1 = 0.0707$ for 14 802 observed data based on $F_o \geq 4.0\sigma(F_o)$ and $R_{2w} = 0.2007$ for 21 696 total unique data. The atomic coordinates are listed in Table 2; the anisotropic thermal parameters and the fixed hydrogen atom coordinates are included in the Supporting Information (Tables S2 and S3).

**Magnetic Susceptibilities.** Crystalline $\{[Mn(TPP)]_2(OH)\}ClO_4$ from $CH_2Cl_2$ and hexanes was harvested and crushed to powder. The powder sample was dried under vacuum for ~3 h and was then used to measure the magnetic susceptibilities in both solution and solid state.

The Evans NMR method was used to obtain solution magnetic susceptibilities.[21] A $CDCl_3$ solution of the crushed crystal sample (0.2 mL, $c = 3.8 \times 10^{-3}$ M) was transferred into the inner tube, and 0.25 mL of $CDCl_3$, into the outer tube. An NMR spectrum was then recorded at 20 °C, and the line shift of $CHCl_3$ was measured to calculate the solution susceptibility.

Solid-state magnetic susceptibilities were measured under helium on a Quantum Design MPMS SQUID susceptometer from 2 to 300 K at a field of 0.5 T. The sample (22.16 mg) was contained in a Kel-F bucket which had been calibrated independently at the same field and temperatures. The raw data file was corrected for the diamagnetic contribution ($1.0 \times 10^{-3}$) of both the sample holder and the compound to the susceptibility. The reported magnetic data[22] for [Mn(TPP)Cl] were used to apply a correction for the paramagnetic impurity.

## Results

**X-ray Structure of $\{[Mn(TPP)]_2(OH)\}ClO_4$.** Figures 2 and 3 are ORTEP diagrams of the $\{[Mn(TPP)]_2(OH)\}^+$ cation. Figure 3 also illustrates the labeling scheme used in the tables for the non-hydrogen atoms. Porphyrin ring 1 (drawn with open bonds) is labeled completely; however, only the *meso*-phenyl carbon and pyrrole nitrogen atoms are labeled for ring 2 (drawn with solid bonds), since its nomenclature is exactly the same as that of ring 1. To further increase the clarity of the diagram, the porphyrin ring indices ("1" and "2"), the "C" for all the carbon atoms, and the parentheses are omitted in the labeling scheme. Selected bond distances and angles are given in Table 3. Complete bond distances and angles are listed in the Supporting Information (Tables S5 and S6). Averaged values for the unique chemical classes of distances and angles in the porphinato cores are entered on the mean-plane diagrams given in Figure 4.

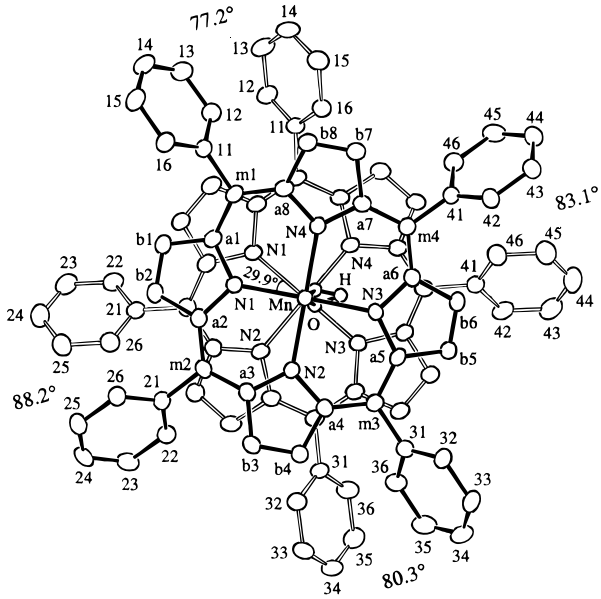


**Figure 3.** "Top-view" ORTEP diagram of $\{[Mn(TPP)]_2(OH)\}^+$ with atom-labeling scheme. The Mn(1)···Mn(2) axis is perpendicular to the plane of the paper. Thermal ellipsoids are drawn at the 50% probability level, except for the thermal parameters of the $\mu$-hydroxo group, which have been reduced by a factor of 2. Porphyrin ring 2 is drawn with solid bonds and completely labeled; while ring 1 is drawn with open bonds and only the labeling scheme for the four phenyl groups are given, those for the 24-atom core are identical to ring 2 after a 30° clockwise rotation and are eliminated for clarity. Both disordered oxygen atoms of the bridging hydroxide are shown.

**Table 3.** Selected Bond Lengths (Å) and Angles (deg) for $\{[Mn(TPP)]_2OH\}ClO_4$[a]

| | | | |
|---|---|---|---|
| Mn(1)−O(1a) | 2.041(5) | Mn(2)−O(1a) | 2.015(5) |
| Mn(1)−O(1b) | 2.009(8) | Mn(2)−O(1b) | 2.040(9) |
| Mn(1)−1N(1) | 1.999(3) | Mn(2)−2N(1) | 2.001(3) |
| Mn(1)−1N(2) | 2.011(3) | Mn(2)−2N(2) | 2.004(3) |
| Mn(1)−1N(3) | 2.007(3) | Mn(2)−2N(3) | 2.006(3) |
| Mn(1)−1N(4) | 2.016(3) | Mn(2)−2N(4) | 2.020(3) |
| O(1a)−H(1) | 0.73(6) | O(1b)−H(1) | 0.77(6) |
| 1N(1)−Mn(1)−O(1a) | 94.6(3) | 2N(1)−Mn(2)−O(1a) | 98.7(2) |
| 1N(2)−Mn(1)−O(1a) | 105.6(3) | 2N(2)−Mn(2)−O(1a) | 102.7(4) |
| 1N(3)−Mn(1)−O(1a) | 96.0(3) | 2N(3)−Mn(2)−O(1a) | 92.3(2) |
| 1N(4)−Mn(1)−O(1a) | 87.8(3) | 2N(4)−Mn(2)−O(1a) | 91.7(4) |
| 1N(1)−Mn(1)−1N(2) | 89.50(12) | 2N(1)−Mn(2)−2N(2) | 89.37(11) |
| 1N(1)−Mn(1)−1N(3) | 169.16(12) | 2N(1)−Mn(2)−2N(3) | 169.06(12) |
| 1N(1)−Mn(1)−1N(4) | 89.61(12) | 2N(1)−Mn(2)−2N(4) | 89.58(11) |
| 1N(2)−Mn(1)−1N(3) | 89.88(12) | 2N(2)−Mn(2)−2N(3) | 88.91(11) |
| 1N(2)−Mn(1)−1N(4) | 166.57(12) | 2N(2)−Mn(2)−2N(4) | 165.63(12) |
| 1N(3)−Mn(1)−1N(4) | 88.49(12) | 2N(3)−Mn(2)−2N(4) | 89.40(11) |
| Mn(1)−O(1a)−Mn(2) | 159.8(5) | | |
| Mn(1)−O(1b)−Mn(2) | 160.9(8) | | |

[a] Estimated standard deviations of the least significant digits are given in parentheses.

The average $Mn-N_p$ bond distances in the two porphinato cores are identical at $Mn(1)-N_p = 2.008(7)$ and $Mn(2)-N_p = 2.008(8)$ Å, where the numbers in parentheses are the esd's of the average. The two manganese ions are displaced by 0.19 and 0.20 Å from their respective 24-atom mean planes and 0.21

(20) $R_1 = \sum||F_o| - |F_c||/\sum|F_o|$ and $R_{2w} = \{\sum[w(F_o^2 - F_c^2)^2]/\sum[wF_o^4]\}^{1/2}$. The conventional $R$ factors $R_1$ are based on $F$, with $F$ set to zero for negative $F^2$. The criterion of $F^2 > 2\sigma(F^2)$ was used only for calculating $R_1$. $R$ factors based on $F^2$ ($R_{2w}$) are statistically about twice as large as those based on $F$, and $R$ factors based on ALL data will be even larger. The values given in Table 1 are for the 14 802 observed data. Values for all unique data (21 696) are $R_1 = 0.1127$ and $R_{2w} = 0.2007$.

(21) (a) Evans, D. F. *J. Chem. Soc.* **1959**, 2003. (b) Bartle, K. D.; Dale, B. J.; Jones, D. W.; Maricic, S. J. *Magn. Reson.* **1973**, *12*, 286.

(22) Behere, D. V.; Mitra, S. *Inorg. Chem.* **1980**, *19*, 992.

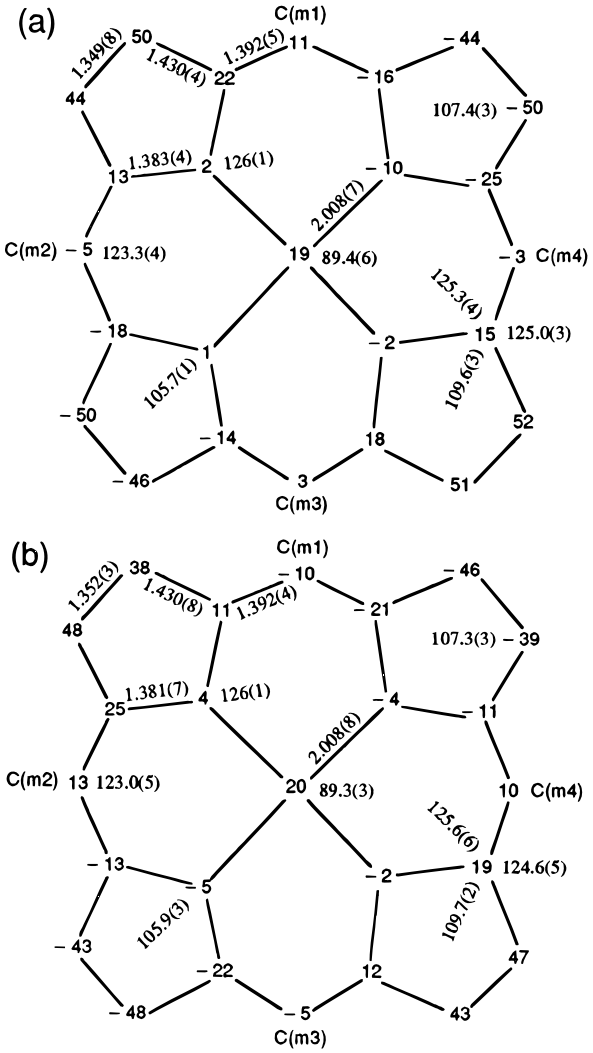


**Figure 4.** Formal diagrams of the porphinato cores of $\{[Mn(TPP)]_2(OH)\}ClO_4$ for porphyrin ring 1 (a) and for ring 2 (b), displaying the average values for the bond parameters in each ring. The value for the perpendicular displacement of each atom (in units of 0.01 Å) of the 24-atom core of both rings is shown. For both rings, a positive value is a displacement toward the other ring of the dimer.

and 0.22 Å from their respective four-pyrrole-nitrogen mean planes, each toward the bridging hydroxide group. The Mn(1)···Mn(2) separation is 3.993(2) Å. The oxygen atom of the $\mu$-hydroxo ligand is disordered at two positions (O(1a) and O(1b)) with a separation of 0.42 Å, while only one hydrogen atom can be located from the difference Fourier with distances to O(1a) and O(1b) of 0.73(6) and 0.77(6) Å, respectively. It can be seen from Figure 3 that the direction of this disorder (the O(1a)···O(1b) vector) is nearly perpendicular to the plane defined by Mn(1), Mn(2), and the $\mu$-hydroxo hydrogen atom. Therefore the geometries of the two Mn−O(H)−Mn entities are nearly identical.[23] The distances between the disordered oxygen positions to the Mn(III) centers have average values of 2.025(23) Å (to Mn(1)) and 2.028(18) Å (to Mn(2)), and the average Mn−O(H)−Mn bridging angle is 160.4(8)°. The average values for the O−Mn−$N_p$ angle are 96.0(6.1)° for Mn(1) and 96.3(5.6)° for Mn(2). The N−Mn−Mn′−N′ dihedral angles have an average value of 29.9(6)°. The two porphyrin rings are found to be nearly parallel to each other with dihedral angles of only 4.0 and 6.4° between the mean planes of the 24-atom cores and four-nitrogen cores, respectively. Each of the phenyl groups of one porphyrin ligand is found to form a pair with a phenyl group of another porphyrin ligand (see Figure 2). The two phenyl rings within a pair are nearly perpendicular to each other with observed Ph−Ph dihedral angles of 77.2, 88.2, 80.3, and 83.1°.

(23) In other $\mu$-hydroxo structures,[9,7,24] we have found that the H atom is out of the plane defined by M(1), M(2), and O, although the displacement in the present case is somewhat larger. Hence it is reasonable to believe that the H atom is also disordered but with a H···H separation less than 0.42 Å value of the two oxygen atoms.

(24) The analogous single $\mu$-hydroxo complexes $\{[M(OEP)]_2OH\}ClO_4$ with M = Ga(III) and In(III) have been synthesized and structurally characterized: Chen, B.; Scheidt, W. R. Manuscript in preparation.

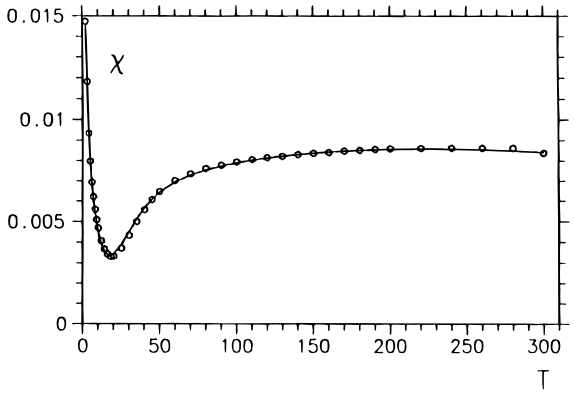


**Figure 5.** Temperature dependence of the magnetic susceptibility for a powder sample of $\{[Mn(TPP)]_2(OH)\}ClO_4$. The solid line was calculated with the following set of parameters: $2J = -74.0$ cm$^{-1}$, $D = -10.8$ cm$^{-1}$. The mole fraction of a monomeric, $S = 2$, impurity with ZFS equal to $-2.3$ cm$^{-1}$ was adjusted to $w_{mo} = 1.35\%$. The value of $g$ was taken as 2.0 for the dimer and the monomeric impurity.

**Magnetism.** The detailed methodology of the analysis of the temperature-dependent magnetic susceptibilities was described previously.[9] The temperature dependence of $\chi$ for a powder sample of $\{[Mn(TPP)]_2(OH)\}ClO_4$ is shown in Figure 5. The observed behavior is typical of an exchange-coupled dinuclear complex containing a small residual mononuclear impurity, which is assumed to be [Mn(TPP)Cl]. The data were fit to the total spin Hamiltonian of a zero-field-split, high-spin $d^4-d^4$ dimer, including a monomeric $S = 2$ impurity. In view of the axially elongated structure around Mn(III) in the dimer, a negative sign is expected for $D$;[9] thus $D$ was constrained to negative values in our calculations. A satisfactory fit is obtained with parameters of $2J = -74.0$ cm$^{-1}$; $D = -10.8$ cm$^{-1}$, and $w_{mo} = 1.35\%$ for a Curie-like impurity.

The solution susceptibility measured by NMR methods in $CDCl_3$ gives a value of 3.3 $\mu_B$ for the effective magnetic moment at 20 °C. This value corresponds[25] to an antiferromagnetic coupling constant $2J$ of $-67.4$ cm$^{-1}$, in satisfactory agreement with the results from solid-state measurements.

## Discussion

**Synthesis.** We previously reported[9] the synthesis, structure, and magnetic characterization of $\{[Mn(OEP)]_2(OH)\}ClO_4$. This hydroxo-bridged species is stable in halocarbon solvents and is readily obtained by a controlled hydrolysis of the monomeric precursor $[Mn(OEP)(H_2O)]ClO_4$ or $[Mn(OEP)(OClO_3)]$. This is in distinct contrast to our observations concerning a related

(25) In order to estimate the coupling constant $J$, a "one-parameter-fit" procedure was applied using the equation

$$\chi_A = \frac{3K}{T}\left[\frac{30 + 14x^8 + 5x^{14} + x^{18}}{9 + 7x^8 + 5x^{14} + 3x^{18} + x^{20}}\right]$$

where $x = \exp(-J/kT)$ and $K = Ng^2\beta^2/3K$. Of course, such a procedure is not guaranteed to produce a coupling constant $J$ with sufficient reliability.

compound: the $\mu$-oxo-bridged species $[Mn(OEP)]_2O$, which appears to be extremely unstable in halocarbon solvents. Attempted synthesis of $[Mn(OEP)]_2O$ with methods that are appropriate for the preparation of $[Fe(OEP)]_2O$[26] were unsuccessful. Although the formation of a new species was indicated by electronic spectra, we were unable to isolate this compound in crystalline form. Recrystallization of "$[Mn(OEP)]_2O$" from $CH_2Cl_2$ or $CHCl_3$ leads exclusively to crystalline [Mn(OEP)Cl]. Attempted crystallization from benzene, toluene, or THF solution were unsuccessful. The difference in hydroxo- vs oxo-bridged species in susceptibility to nucleophilic attack is somewhat unexpected. The difference in stability is also surprising since the Mn−O−Mn angle at the bridging hydroxide is expected to be much more nonlinear than in the oxo derivative and thus more open to attack. Such strong nonlinearity has been observed not only in $\{[Mn(OEP)]_2(OH)\}ClO_4$[9] but also in $\{[Fe(OEP)]_2(OH)\}ClO_4$[7] and the group 13 OEP derivatives,[24] all of which have the two porphyrinato rings strongly canted with respect to each other.

We have now extended our study to this interesting apparent bridging hydroxo vs oxo stability difference to the manganese(III) tetraphenylporphyrinate derivatives. We thought that the use of tetraphenylporphyrin as the porphyrin ligand instead of octaethylporphyrin would enhance the stability of the $\mu$-oxo derivative, since the bulky *meso*-phenyl groups should limit the close approach of the two porphyrin rings, a feature which appeared necessary in order to form the nonlinear hydroxide bridge. Indeed, it was not clear that the $\mu$-hydroxo $Mn^{III}TPP$ complex could be formed at all, considering the structural requirements.

The expected stabilizing steric effects notwithstanding, $[Mn(TPP)]_2O$ does not seem to be any more readily prepared than the OEP derivative, at least as a crystalline solid. In our hands, the reported preparation of "$[Mn(TPP)]_2O$"[27] with pyridine as solvent was not successful; the product was found to be the bis(pyridine) adduct.[28] However, the $\mu$-hydroxo $Mn^{III}TPP$ complex can be reproducibly synthesized by the controlled hydrolysis of the previously reported mononuclear, six-coordinate manganese(III) tetraphenylporphyrinate $[Mn(TPP)(H_2O)_2]ClO_4$.[29]

The hydrolysis of the diaquo precursor can be conveniently monitored by electronic spectra, since the blue shift of the Soret band is a "fingerprint" for the formation of the $\mu$-hydroxo species. Spectra showing the diaquo precursor, an intermediate stage in the hydrolysis, and the final product are given in Figure 6. It can be seen clearly that the Soret band is blue-shifted from 478 nm (the diaquo precursor) to 464 nm (the $\mu$-hydroxo complex). Most importantly, the spectrum of the hydrolysis product is essentially identical to that of the isolated single crystal of $\{[Mn(TPP)]_2(OH)\}ClO_4$, as shown in Figure 1. The biphasic hydrolysis of $[Mn(TPP)(H_2O)_2]ClO_4$ is an efficient method for the synthesis of the $\{[Mn(TPP)]_2(OH)\}ClO_4$ complex. A bulk sample so prepared has a low level of apparent mononuclear impurity as judged by the magnetic susceptibility measurements.

**Structure.** The coordination group geometry of the manganese(III) ions in $\{[Mn(TPP)]_2(OH)\}ClO_4$ is that of a high-spin five-coordinate manganese(III) system. Thus, the averaged value of the $Mn-N_p$ bond distance (2.008(7) Å) and the manganese atom displacement from the 24-atom mean plane (0.20 Å) are within the range expected for high-spin five-coordinate manganese(III) porphyrinates.[9,29,30] The identity of the bridging ligand as the hydroxide ion is confirmed by the stoichiometry, which shows that the binuclear unit is a monocation; the location and refinement of the hydroxide ion hydrogen atom from the X-ray data add additional support to the identification. The average axial Mn−O(H) bond distance of 2.026(17) Å is very close to the 2.011(18) Å value observed for $\{[Mn(OEP)]_2(OH)\}ClO_4$ and consistent with a bridging hydroxide ligand rather than a bridging oxo ligand, whose expected values are in the range 1.78−1.84 Å. The bridging Mn−O(H)−Mn angle of 160.4(8)° is, to our knowledge, the largest value reported for a $\mu$-hydroxo bridge angle.

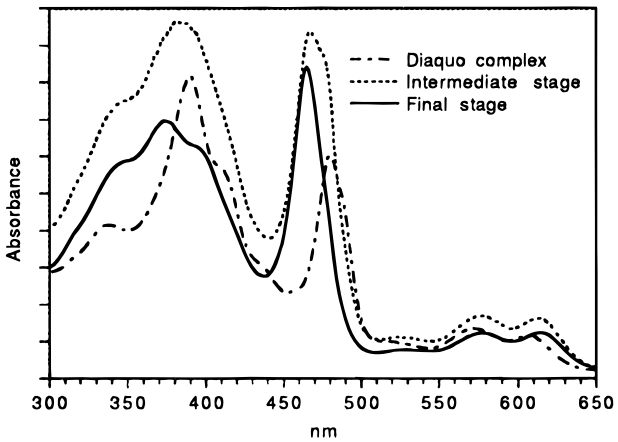


**Figure 6.** Electronic spectra monitoring the synthesis of $\{[Mn(TPP)]_2(OH)\}ClO_4$ from $[Mn(TPP)(H_2O)_2]ClO_4$. Concentrations of all species are arbitrary and were chosen to emphasize the shifts in the spectra.

Our structure determinations of several hydroxo-bridged octaethylporphyrin derivatives[7,9,24] led us to expect that a tetraphenylporphyrin derivative would be very sterically stressed. There appear to be two contradictory structural requirements in the hydroxide-bridged species. In order of apparent importance these are (i) to make the bridging hydroxide angle as small as possible while (ii) also minimizing the intramolecular porphyrin−porphyrin interactions. In the OEP derivatives, the two porphyrin rings are canted with respect to each other in order to accommodate the nonlinear M−O(H)−M angle. The interplanar angle in the OEP derivatives is limited by the closest approach of the rings (~3.3 Å spacing). In the TPP system, the inter-ring interactions of the peripheral *meso*-phenyl groups must also be taken into account. This factor is expected to limit the dihedral angle between the two porphyrin planes to values near zero. Indeed, the observed dihedral angle between the two 24-atom mean planes is only 4.0° while the value between the two $N_4$ mean planes is 6.4°, suggestive of a significant, strong interaction between the two porphyrin rings. Nevertheless, despite the near coplanarity of the two rings, the Mn−O(H)−Mn bond angle is still decidedly nonlinear at 160.4(8)°.

Obviously, the two Mn−O(H) vectors cannot be perpendicular to the porphyrin mean planes but must be offset to

(26) Cohen, I. A. *J. Am. Chem. Soc.* **1969**, *91*, 1980. La Mar, G. N.; Eaton, G. R.; Holm, R. H.; Walker, F. A. *J. Am. Chem. Soc.* **1973**, *95*, 63.
(27) Fleischer, E. B.; Palmer, J. M.; Srivastava, T. S.; Chatterjee, A. *J. Am. Chem. Soc.* **1971**, *93*, 3162.
(28) Cheng, B. Unpublished results.
(29) (a) Kennedy, B. J.; Murray, K. S. *Inorg. Chem.* **1985**, *24*, 1557. (b) Williamson, M. M.; Hill, C. L. *Inorg. Chem.* **1987**, *26*, 4155.
(30) (a) Day, V. W.; Stults, B. R.; Tasset, E. L.; Marianelli, R. S.; Boucher, L. J. *Inorg. Nucl. Chem. Lett.* **1975**, *11*, 505. (b) Tulinsky, A.; Chen, B. M. L. *J. Am. Chem. Soc.* **1977**, *99*, 3647. (c) Anderson, O. P.; Lavallee, D. K. *Inorg. Chem.* **1977**, *16*, 1634. (d) Scheidt, W. R.; Lee, Y. J.; Luangdilok, W.; Haller, K. J.; Anzai, K.; Hatano, K. *Inorg. Chem.* **1983**, *22*, 1516. (e) Williamson, M. M.; Hill, C. L. *Inorg. Chem.* **1986**, *26*, 4668. (f) Jinghe, Z.; Shongchun, J.; Zhungsheng, J.; Rizhen, J. *Chin. J. Appl. Chem.* **1988**, *5*, 50. (g) Suslick, K. S.; Watson, R. A. *Inorg. Chem.* **1991**, *30*, 912. (h) Suslick, K. S.; Watson, R. A.; Wilson, S. R. *Inorg. Chem.* **1991**, *30*, 2311. (i) Armstrong, R. S.; Foran, G. J.; Hambley, T. W. *Acta Crystallogr., Sect. C* **1993**, *C49*, 236.

**Table 4.** Selected Structural Features for Monobridged Binuclear Porphinato Complexes

| compound | interplanar angle,[a] deg | mean-plane sepn,[b] Å | twist angle,[c] deg | dihedral angle, deg[d] phenyl−phenyl distance, Å | | | | average[d] | ref |
|---|---|---|---|---|---|---|---|---|---|
| $[Fe(TF_5PP)]_2O$ | 1.6 | 4.9 | 43 | 31.2 | 35.5 | 41.4 | | 37.4 | 34 |
| | | | | 6.64 | 6.85 | 6.95 | | 6.85 | |
| $[Fe(TPP)]_2O$ | 3.7 | 4.50 | 35.4 | 28.0 | 27.8 | 35.5 | | 31.7 | 35 |
| | | | | 6.46 | 6.04 | 5.81 | | 6.03 | |
| $[Fe(TPP)]_2N$ | 0.0 | 4.1 | 31.7 | 65.3 | | | | 65.3 | 36 |
| | | | | 5.77 | | | | 5.77 | |
| $[Fe(TPC)]_2O$ | 0.0 | 4.60 | 30.2 | 59.2 | 56.9 | | | 58.0 | 37 |
| | | | | 5.64 | 5.87 | | | 5.76 | |
| $[Fe(TPP)]_2C$ | 0.0 | 3.87 | 31.7 | 66.5 | | | | 66.5 | 38 |
| | | | | 5.75 | | | | 5.75 | |
| $[Mo(TPP)(O)]_2O$ | 0.0 | 3.85 | 30.4 | 70.5 | 75.2 | | | 72.8 | 39 |
| | | | | 5.60 | 5.29 | | | 5.44 | |
| $[Ru(TPP)(p\text{-}OC_6H_4CH_3)]_2O$ | 2.5 | 3.8 | 27.9 | 86.5 | 67.1 | 37.6 | 76.0 | 76.5 | 40 |
| | | | | 5.05 | 5.68 | 5.78 | 5.25 | 5.44 | |
| $[Mo(TTP)(Cl)]_2O$ | 1.6 | 4.01 | 30.4 | 70.1 | 71.8 | 68.7 | 72.5 | 70.8 | 41 |
| | | | | 5.45 | 5.08 | 5.58 | 5.32 | 5.36 | |
| $[Mn(TPP)(N_3)]_2O$ | 0.0 | 3.88 | 28.5 | 85.0 | 61.3 | | | 73.2 | 42 |
| | | | | 4.94 | 5.76 | | | 5.35 | |
| $[Fe(TMPyP)]_2O\cdot(ClO_4)_8$ | 0.4 | 4.43 | 32.4 | 68.7 | 62.9 | | | 65.8 | 43 |
| | | | | 5.42 | 5.23 | | | 5.32 | |
| $[(NCH_3TPP)Fe-O-Fe(TPP)]ClO_4$ | 1.6 | 4.4 | 30.2 | 85.8 | 82.3 | 69.2 | 79.3 | 79.2 | 44 |
| | | | | 5.10 | 5.15 | 5.42 | 5.44 | 5.28 | |
| $[Fe(FF)]_2O\cdot H_2O$ | 15.8 | 4.7 | 24 | 4.6 | 61.8 | 67.2 | 42.3 | 57.1 | 45 |
| | | | | 7.67 | 5.09 | 5.26 | 5.19 | 5.18 | |
| $\{[Mn(TPP)]_2OH\}ClO_4$ | 3.96 | 4.38 | 29.9 | 77.2 | 88.2 | 80.3 | 83.1 | 82.2 | this |
| | | | | 4.87 | 4.93 | 5.49 | 5.31 | 5.15 | work |

[a] The dihedral angle of two mean planes of the 24-atom cores within a dimeric molecule. [b] The average separation of individual atom from the other 24-atom core. [c] Average of the four N−M−M′−N′ dihedral angles. [d] The top line is the dihedral angle between the two phenyl rings, and the lower line is the corresponding center−center distance.

accommodate the ∼16° difference. Indeed the eight $N_p$−Mn−O(H) angles range from 87.8(3) to 105.6(3)°. Interestingly, the dihedral angle between the porphyrin planes in the Mn, Fe, and Ga OEP systems is also ∼15° smaller than that predicted from consideration of the M−O(H)−M angle.[31] In all systems, the strain in the required off-normal axial bond vectors is taken up more by one metal than the other in the binuclear complexes. We do conclude that the relatively large values of the M−O(H)−M bond angle in all systems is dominated by intramolecular inter-ring steric repulsion factors, with the largest value found for the TPP system.

There are a number of other interesting structural features found for the $\{[Mn(TPP)]_2(OH)\}ClO_4$ molecule. Some, but not all, are related to minimizing the intra- and intermolecular *meso* phenyl−phenyl interactions. The separation between the two porphyrin mean planes is 4.4 Å, and the inter-ring twist angle is found to be 29.9° (see Figure 3). The twist angles in the OEP derivatives are much smaller and would lead to close inter-ring phenyl ring contacts. The two porphyrin cores exhibit substantial $D_{2d}$-ruffled cores of the *sad* type[8,32] as can be seen in Figure 4. However, the saddle core conformations do not appear to result from *intra*molecular interactions but rather from "dimeric" intermolecular interactions that Scheidt and Lee[32] noted led to *sad* core conformations. These interactions are relatively tight for both rings of $\{[Mn(TPP)]_2(OH)\}ClO_4$, and both inter-ring interactions are between rings related by inversion centers. For ring 1, there is a separation between the two mean planes of 3.51 Å, a lateral shift of 3.51 Å, and a slip angle of 45.0°. The corresponding values involving ring 2 are 3.61 Å, 3.69 Å, and 45.6°. Values for a number of analogous ring−ring interactions in other tetraarylporphyrin systems were gathered in Table XXIV of ref 32.

As was noted previously,[32] the *sad* ruffling results from relatively small dihedral angles between the mean plane of the porphyrin core and the peripheral phenyl groups. This structural feature arises from attempting to make the entire tetraphenylporphyrin moiety as coplanar as possible in order to allow the intermolecular close approach of two such groups. The values of the eight dihedral angles range from 47.1 to 54.8°, with an average value of 51(3)°. Perhaps surprisingly, the effects of the *sad* ruffling do not appear to decrease the intramolecular, inter-ring distances between the atoms that define the two 24-atom cores. Rather, the $S_4$-ruffling of the cores leads to the pyrrole rings of the two cores alternatively tipping toward each other or away from each other. This leads to the closest pair of atom−atom contacts at 3.38 Å. Indeed, this distance is comparable to the shorest such inter-ring distance observed in the OEP derivatives, where the close contact between the two rings results from the canting of the two cores.

It might have been expected that the closest intramolecular pairs of phenyl rings in $\{[Mn(TPP)]_2(OH)\}ClO_4$ would have parallel or nearly parallel relative orientations, in order to minimize the phenyl−phenyl nonbonded interactions. However, the four pairs of phenyl rings have nearly perpendicular orientations with Ph−Ph dihedral angles of 77.2, 88.2, 80.3, and 83.1° (see Figure 3). This interesting structural feature led us to examine the relative phenyl ring−phenyl ring orientations for all previously reported binuclear tetraarylporphyrin systems with a single oxygen, nitrogen, or carbon atom as the bridging ligand. The values of the phenyl−phenyl dihedral angles and selected other structural features are given in Table 4. Values range upward from 30°, but a number of derivatives have phenyl ring pairs with relative perpendicular orientations. However, there does not seem be any correlation between the Ph−Ph dihedral angle values and a number of other structural parameters such as the dihedral angle between the two porphyrin planes, the porphyrin mean plane separation, and the $N_p$−M−

(31) The predicted dihedral angle is [180 − (the M−O(H)−M angle)]°.

(32) Scheidt, W. R.; Lee, Y. J. Recent Advances in the Stereochemistry of Metallotetrapyrroles. *Struct. Bonding (Berlin)* **1987**, *64*, 1.

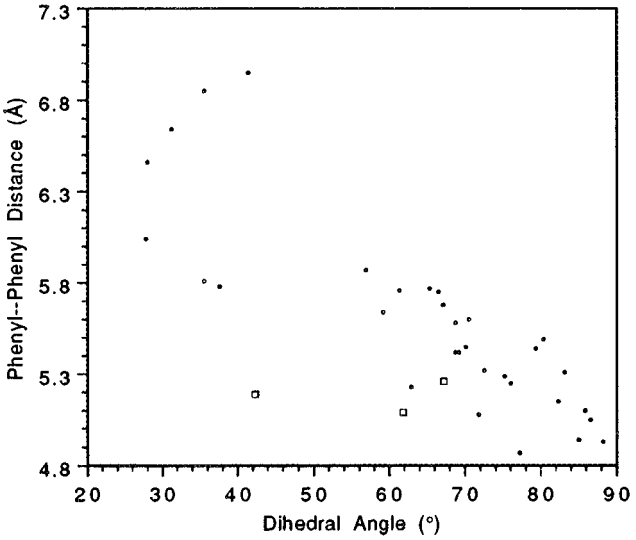


**Figure 7.** Plot of the center to center distances of the phenyl rings vs the Ph−Ph dihedral angles listed in Table 4.

M′−$N_p$′ dihedral angles (the twist angles). These parameters might be thought to bear some relation to phenyl ring interactions. A correlation does exist between the Ph−Ph orientation and the center to center distance within a pair of phenyl rings. Figure 7 is a plot of all observed Ph−Ph dihedral angles vs the phenyl center−center distances. It can be clearly seen that the dihedral angles fall into two groups that are separated by a gap of almost 20°. Furthermore, it is quite clear that as pairs of phenyl rings become closer, the phenyl group orientations tend toward 90°. Thus as the distance between a pair of phenyl rings become smaller, the two rings adopt a geometry in which they become nearly perpendicular. It should be noted that while, to a good approximation, the phenyl ring orientations do not have any effect on the center−center distance, all of the geometric parameters listed in Table 4 collectively have an effect on phenyl ring pair separations. We do note a special case, $[Fe(FF)]_2O$,[45] in which the porphyrin macrocycles are covalently linked through two *ortho*-substituted phenyl rings with a urea bridge. The consequent geometry might appear to favor all phenyl ring pairs being nearly parallel. However, even in this case, the center−center distance trend seems to be followed. The values for this special case are marked with the open symbols in Figure 7. There thus appears to be a favored orientation of the phenyl rings that is dependent only on the center−center distance. Indeed, theoretical calculations[33] have suggested that perpendicular orientations are preferred when two phenyl rings lie above each other.

The hydroxide ion is in a very unusual chemical environment, similar to that found for $\{[Mn(OEP)]_2(OH)\}ClO_4$ and the analogous iron complex. All of the close contacts found between the oxygen or hydrogen atom of the hydroxide ion are with atoms of the porphyrin rings. The hydroxide ion and the perchlorate ion are well separated, with a shortest O···O distance of 8.2 Å. However, the hydroxide hydrogen atom is within hydrogen-bonding distance of the porphyrin nitrogen atom 2N(3) at a distance of 2.49 Å with a 2N(3)−H−O angle of 114°.

The solvent content (and crystallographic model) of the $\{[Mn(TPP)]_2(OH)\}ClO_4$ lattice is complex. The symmetry-unique portion of the lattice has six different solvent regions (holes). Four of these contain methylene chloride molecules solely, although not necessarily at full occupancy. The remaining two solvent holes appear to contain either methylene chloride or water. Our model for water is based on a fit of the electron density and the observation that water molecules in the two regions are within hydrogen-bonding distance of each other. The crystalline lattice appears to be quite unstable; loss of crystallinity occurs quite rapidly when crystals are removed from mother liquor. Crystals must first be embedded in silicone grease in the crystallizing medium and then quickly transferred to the nitrogen cold stream on the diffractometer for data collection.

**Magnetic Properties.** The temperature-dependent magnetic susceptibility of $\{[Mn(TPP)]_2(OH)\}ClO_4$ (Figure 5) has been well fit by assuming an antiferromagnetic exchange coupling between two $S = 2$ Mn(III) centers mediated by the single bridging hydroxo ligand. The antiferromagnetic coupling constant ($2J = -74.0$ cm$^{-1}$) found for this molecule is marginally larger than that found for $\{[Mn(OEP)]_2(OH)\}ClO_4$ ($2J = -71.0$ cm$^{-1}$).[9] If the marginal difference is real, it is consistent with the expectation that the larger hydroxide bridging angle (160.4°) in $\{[Mn(TPP)]_2(OH)\}ClO_4$ should lead to a larger value of the coupling constant, since stronger antiferromagnetic coupling is found as the M−O−M bridge angle becomes larger.[46] Compared to the case of binuclear Mn(III) Schiff base complexes with a single hydroxo bridging ligand, the antiferromagnetic coupling in $\{[Mn(TPP)]_2(OH)\}ClO_4$ is significantly stronger than that of ($\mu$-hydroxo)bis($\mu$-acetato)dimanganese(II)[47] and two Mn(IV) tetramers,[48] where the coupling constants are $2J = -18$ and $-40$ to $-44$ cm$^{-1}$, respectively. The marginally larger value of the zero-field splitting in the TPP derivative compared to the OEP derivative[9] ($D = -10.8$ vs $-8 \pm 2$ cm$^{-1}$) is consistent with the larger axial elongation around manganese(III) in the former.

**Summary.** The synthesis of the hydroxo-bridged complex $\{[Mn(TPP)]_2(OH)\}ClO_4$ through a controlled hydrolysis of $[Mn(TPP)(H_2O)_2]^+$ is demonstrated. The X-ray structure shows that each Mn(III) ion is axially coordinated with a Mn−O(H)−Mn bridge angle of about 160° and nearly coplanar porphyrin rings.

(33) (a) Pawliszyn, J.; Szezesniak, M. M.; Scheiner, S. *J. Phys. Chem.* **1984**, *88*, 1726. (b) Karlstrom, G.; Linse, P.; Wallquist, A.; Jönsson, B. *J. Am. Chem. Soc.* **1983**, *105*, 3777.
(34) Gold, A.; Jayaraj, K.; Doppelt, P.; Fischer, J.; Weiss, R. *Inorg. Chim. Acta* **1988**, *150*, 177.
(35) (a) Hoffman, A. B.; Collins, D. M.; Day, V. W.; Fleischer, E. B.; Srivastava, T. S.; Hoard, J. L. *J. Am. Chem. Soc.* **1972**, *94*, 3620. (b) Swepston, P. N.; Ibers, J. A. *Acta Crystallogr., Sect. C* **1985**, *C41*, 671.
(36) Scheidt, W. R.; Summerville, D. A.; Cohen, I. A. *J. Am. Chem. Soc.* **1976**, *98*, 6623.
(37) Strauss, S. H.; Pawlik, M. J.; Skowyra, J.; Kennedy, J. R.; Anderson, O. P.; Spartalian, K.; Dye, J. L. *Inorg. Chem.* **1987**, *26*, 724.
(38) Goedken, V. L.; Deakin, M. R.; Bottomley, L. A. *J. Chem. Soc., Chem. Commun.* **1982**, 607.
(39) (a) Johnson, J. F.; Scheidt, W. R. *J. Am. Chem. Soc.* **1977**, *99*, 294. (b) Johnson, J. F.; Scheidt, W. R. *Inorg. Chem.* **1978**, *17*, 1280.
(40) Collman, J. P.; Barnes, C. E.; Brothers, P. J.; Collins, T. J.; Ozawa, T.; Gallucci, J. C.; Ibers, J. A. *J. Am. Chem. Soc.* **1984**, *106*, 5151.
(41) Colin, J.; Chevrier, B.; De Cian, A.; Weiss, R. *Angew. Chem., Int. Ed. Engl.* **1983**, *22*, 247.
(42) (a) Schardt, B. C.; Hollander, F. J.; Hill, C. L. *J. Chem. Soc., Chem. Commun.* **1981**, 765. (b) Schardt, B. C.; Hollander, F. J.; Hill, C. L. *J. Am. Chem. Soc.* **1982**, *104*, 3964.
(43) Ivanca, M. A.; Lappin, A. G.; Scheidt, W. R. *Inorg. Chem.* **1991**, *30*, 711.
(44) Bartczak, T. J.; Latos-Grazynski, L.; Wyslouch, A. *Inorg. Chim. Acta* **1990**, *171*, 205.
(45) Landrum, J. T.; Grimmett, D.; Haller, K. J.; Scheidt, W. R.; Reed, C. A. *J. Am. Chem. Soc.* **1981**, *103*, 2640.
(46) Such a relationship for bridging hydroxo has perhaps been best shown for copper(II) species: Hodgson, D. K. In *Progress in Inorganic Chemistry*; Lippard, S. J., Ed.; Interscience: New York, 1975; Vol. 19, Chapter 4.
(47) Bossek, U.; Wieghardt, K.; Nuber, B.; Weiss, J. *Inorg. Chim. Acta* **1989**, *165*, 123.
(48) Hagen, K. S.; Westmoreland, T. D.; Scott, M. J.; Armstrong, W. H. *J. Am. Chem. Soc.* **1989**, *111*, 1907.

These features result from the steric constraints of the hindered tetraphenylporphyrin ligand. Steric crowding also leads to phenyl ring pairs that are nearly perpendicular to each other. Temperature-dependent magnetic susceptibility measurements show that the Mn(III)···Mn(III) exchange interaction is moderately antiferromagnetic ($2J = -74.0$ cm$^{-1}$) and modulated by zero-field-splitting effects.

**Acknowledgment.** We thank the National Institutes of Health for support of this research under Grant GM-38401 to W.R.S. Funds for the purchase of the FAST area detector diffractometer were provided through NIH Grant RR-06709.

**Supporting Information Available:** Tables S1−S3, giving complete crystallographic details, anisotropic thermal parameters, and fixed hydrogen atom coordinates for {[Mn(TPP)]$_2$(OH)}ClO$_4$, Table S4, giving magnetic susceptibility data for {[Mn(TPP)]$_2$(OH)}ClO$_4$, and Tables S5 and S6, listing complete bond distances and angles (14 pages). Ordering information is given on any current masthead page.

IC951041C